Exciton diffusion length in narrow bandgap polymers

Mikhnenko, Oleksandr V.; Azimi, Hamed; Scharber, Markus; Morana, Mauro; Blom, Paul W. M.; Loi, Maria Antonietta

IMPORTANT NOTE: You are advised to consult the publisher's version (publisher's PDF) if you wish to cite from it. Please check the document version below.

Document Version
Publisher's PDF, also known as Version of record

[Link to publication in University of Groningen/UMCG research database](#)

PAPER

Exciton diffusion length in narrow bandgap polymers

Oleksandr V. Mikhnenko,*[ab] Hamed Azimi,[c] Markus Scharber,[c] Mauro Morana,[c] Paul W. M. Blom[ad] and Maria Antonietta Loi*[a]

We developed a new method to accurately extract the singlet exciton diffusion length in organic semiconductors by blending them with a low concentration of methanofullerene[6,6]-phenyl-C_{61}-butyric acid methyl ester (PCBM). The dependence of photoluminescence (PL) decay time on the fullerene concentration provides information on both exciton diffusion and the nanocomposition of the blend. Experimentally measured PL decays of blends based on two narrow band gap dithiophene–benzothiadiazole polymers, C–PCPDTBT and Si–PCPDTBT, were modeled using a Monte Carlo simulation of 3D exciton diffusion in the blend. The simulation software is available for download. The extracted exciton diffusion length is 10.5 ± 1 nm in both narrow band gap polymers, being considerably longer than the 5.4 ± 0.7 nm that was measured with the same technique in the model compound poly(3-hexylthiophene) as a reference. Our approach is simple, fast and allows us to systematically measure and compare exciton diffusion length in a large number of compounds.

1. Introduction

Organic semiconductors are very interesting for material research since they can be structurally manipulated by means of organic synthesis to achieve better performances in optoelectronic devices. In the last few years the external power conversion efficiency of organic solar cells has been almost doubled from 4–5% (ref. 1) up to 8.3% (ref. 2) by synthesizing new narrow band gap materials but keeping the same device structure. However, it is not entirely clear what physical properties make the performance of these new materials better. More knowledge is needed to understand the design criteria for more efficient materials.

Exciton diffusion is a key process in the operation of organic solar cells.[3] Excitons are bound electron–hole pairs that are created in organic semiconductors by light absorption, and have to be separated into free charges in order to generate photocurrent. Such a separation is normally achieved at the interface with an electron accepting material, for instance PCBM (see Fig. 1). Excitons reach this interface by incoherent hopping that can be described in terms of diffusion. Therefore the characteristic distance that excitons are able to diffuse, the diffusion length, determines the amount of excitons that can contribute to the photocurrent and consequently to the device efficiency. Thus,

[a] Zernike Institute for Advanced Materials, University of Groningen, Nijenborgh 4, 9747 AG Groningen, The Netherlands. E-mail: alex@mikhnenko.com; m.a.loi@rug.nl
[b] Dutch Polymer Institute, P.O. Box 902, 5600 AX Eindhoven, The Netherlands
[c] Konarka Austria Forschungs und Enwicklungs GmbH, Altenbergerstr. 60, 4040 Linz, Austria
[d] Holst Centre, High Tech Campus 31, 5605 KN Eindhoven, The Netherlands

Broader context

Recently the efficiency of bulk heterojunction organic solar cells has been doubled from 4–5% up to 10% by using new materials but keeping the same device structure. However, it is not entirely clear what material properties are responsible for better performances. Systematic studies of these physical properties are needed to understand the key parameters and provide guidelines for the synthesis of even more efficient materials. The exciton diffusion length is one of such parameters. Here we presented a new method to measure exciton diffusion length in organic semiconductors. With this method we extracted the exciton diffusion length in two narrow band gap dithiophene–benzothiadiazole polymers (C–PCPDTBT and Si–PCPDTBT). Moreover, this work answers the question of what is the influence of the Si atom inserted into the polymer backbone on the exciton diffusion. We found that the exciton diffusion coefficient is twofold smaller in Si–PCPDTBT as compared to the carbon bridged material. Remarkably, the exciton diffusion length is the same in both materials. Additionally, this method gives information about the morphology of the polymer–fullerene blends in blends with fullerene concentration from 0.01 to 10 wt%, providing one of the unique tools to test nano-size morphology in organic semiconductor blends.
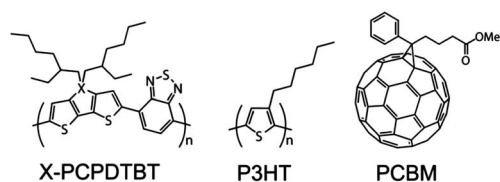
Fig. 1 Chemical structures of poly[2,6-(4,4-bis-(2-ethylhexyl)-4H-cyclopenta[2,1-b; 3,4-b′]dithiophene)-*alt*-4,7-(2,1,3-benzothiadi-azole)] (**C–PCPDTBT**), poly[(4,4′-bis(2-ethylhexyl)dithieno[3,2-b:2′,3′-d]silole)-2,6-diyl-*alt*-(2,1,3-benzothiadiazole)-4,7-diyl] (**Si–PCPDTBT**), poly(3-hexylthiophene) (**P3HT**) and methanofullerene[6,6]-phenyl-C_{61}-butyric acid methyl ester (**PCBM**).

systematic measurements of exciton diffusion length are required to develop the synthetic guidelines for the enhancement of the solar cell efficiency.

Various techniques to measure the exciton diffusion length have been reported in the literature.[3–32] The most popular method is the fluorescence quenching in thin films of organic semiconductors, in which one or both interfaces act as an exciton quenching wall.[4,9,14,19–27,29,31] In this technique the dependence of the exciton quenching efficiency on the semiconductor thickness is measured and modeled with 1D diffusion equation to extract the diffusion length. This is a direct measurement, however it is rather difficult to apply due to many experimental requirements and difficulties in modeling. A sharp boundary is necessary between the semiconductor and the quenching wall.[27] The variation of the exciton density due to optical interference and absorption,[13,31,33] the effect of the polymer–vacuum interface[34] and Forster energy transfer[9,18,31] should be carefully evaluated and taken into account in the modeling. Finally, high precision thickness measurements are needed to accurately determine the exciton diffusion length. Other measurement techniques include exciton density modulation due to light absorption;[15–18,23] exciton–exciton annihilation;[11,13,30] photocurrent modeling in solar cells;[20–22,35] and microwave conductivity.[32] These methods have their advantages and also limitations that are related to the difficulties in sample preparation and/or sophisticated measurement technique, complicated modeling with many fitting parameters, *etc.*

Fluorescence quenching in thin films with randomly distributed quenchers is an interesting approach to measure the exciton diffusion length.[10,12,24,36] If the concentration of quencher sites is well controlled then the comparison of the photoluminescence (PL) decay of the blend with that of the pristine semiconductor gives the value of the exciton diffusion length. On the experimental side, the sample preparation is very simple as well as the measurement of PL decays. However, the analytical model is rather tedious and can be applied only within certain limitations.[12,24,36–39] Furthermore the knowledge about the nano-composition of the blend is required for accurate measurements. Quenching molecules can form phase separated domains, leading to the reduction of the quenching efficiency and underestimation of the exciton diffusion length.

Here we developed a simple method to verify if quencher molecules are intimately mixed or form clusters in the blends with conjugated polymers and accurately evaluate the exciton diffusion length. The technique is based on a Monte Carlo simulation that models PL decays in semiconductor–quencher

mixtures. As interesting testing materials we have chosen the narrow band gap polymers C–PCPDTBT and Si–PCPDTBT that show superior performance in bulk heterojunction solar cells (for full names and chemical structures refer to Fig. 1).[40] We measured for the first time the 3D exciton diffusion length in these polymers, which is the same for both of them and equals to 10.5 ± 1 nm. This value is considerably longer than 5.4 ± 0.7 nm that was measured in P3HT with the same method. Our methodology has numerous advantages compared to other techniques, including simple sample preparation and easy experimental measurements, which allows a systematic study of exciton diffusion length in a large number of materials.

2. Experimental

C–PCPDTBT and Si–PCPDTBT were synthesized by Konarka Technologies; PCBM and regio-regular P3HT were purchased from Solene BV and Sigma-Aldrich, respectively. Solutions of C–PCPDTBT and P3HT in chlorobenzene were mixed with various fractions of PCBM dilute solution, and spin-coated on glass substrates to produce ∼100 nm thick films of polymer–PCBM blends. Si–PCPDTBT was processed from *o*-dichlorobenzene using the doctor blading technique. Samples were prepared under inert nitrogen atmosphere and encapsulated with a glass substrate to further protect films from air during the optical measurements. No annealing steps have been applied to the blends. The C–PCPDTBT- and Si–PCPDTBT-based blends were excited at 760 nm by the principal harmonics of a 100 fs pulsed Ti-sapphire laser. P3HT-based blends were excited at 380 nm by frequency doubled pulses of the same laser. The initial exciton density was kept well below 10^{15} cm^{-3}. PL decays were measured by two Streak cameras sensitive in the near infrared and the visible spectral parts, respectively. The PL decays were spectrally integrated and fitted as mono- or bi-exponential decays for further analysis. Software for Monte Carlo simulations has been specifically developed to model exciton diffusion in polymer–PCBM blends. The Mersenne twister algorithm[41] has been used as a pseudo-random number generator, implemented by A. Fog.[42] The simulation is available for download at ref. 43.

The PCBM volume fraction is the volume occupied by PCBM molecules, which are assumed to be balls with a diameter of 1 nm, divided by the total volume of the blend. The polymer density is an important parameter for determination of the PCBM volume ratio. In our simulation we took a P3HT density of 1.1 g cm^{-3} (ref. 44 and 45). The densities of C–PCPDTBT and Si–PCPDTBT have not been reported yet, however conjugated polymers typically have densities in the range of 0.9–1.4 g cm^{-3} (ref. 44–48). From considerations about the monomer density we found it reasonable to set the polymer density to 1.3 g cm^{-3} in our simulations, resulting in the exciton diffusion length of 10.6 nm. Generally, the fitting results depend only weakly on the polymer density. Thus settings of 1.2 or 1.4 g cm^{-3} in the simulation lead to an exciton diffusion length of 11.1 and 10.2 nm, respectively, giving a change of approximately 0.5 nm per 0.1 g cm^{-3}.

3. Results and discussion

Fig. 2 shows photoluminescence decays of C–PCPDTBT:PCBM blends of various PCBM volume fractions. Higher content of
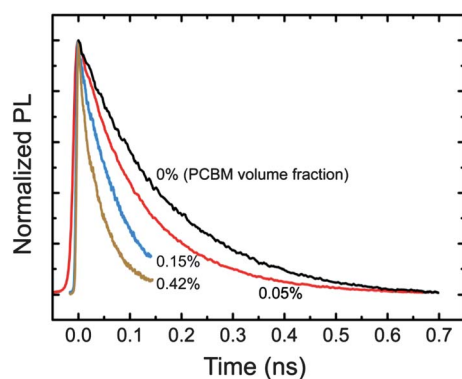
Fig. 2 Measured photoluminescence decays in blends of C–PCPDTBT with PCBM of various volume fractions. The data were normalized to the value at time zero.

PCBM results in shorter PL decay times also in Si–PCPDTBT:PCBM and PH3T:PCBM blends (not shown). The reduction of the PL decay time is a result of the diffusion limited exciton quenching at the polymer–PCBM interface. Considerable quenching is observed when the average distance between PCBM molecules is comparable to—or smaller than—the exciton diffusion length in the polymer phase. In this case the measured PL decay time represents the average diffusion time to quenchers, rather than the natural decay time.

The PL decay time strongly depends on the nanocomposition of the polymer–PCBM blends. For a certain volume fraction of PCBM, the largest quenching surface—consequently the shortest PL decay time—is achieved when PCBM molecules intimately mix with the polymer matrix and form a homogeneous spatial distribution. If the quencher molecules cluster together in phase separated domains, then the PL decay will show a slower dynamics due to the reduction of the quenching surface. To model exciton diffusion in the polymer–PCBM blends it is therefore very important to be aware of the nanocomposition in the blend.

We developed a Monte Carlo simulation of 3D exciton diffusion in a medium with a morphology of arbitrary complexity, including intimate mixture and clustered quencher distribution. Non-interacting excitons undergo a random walk in this medium and decay non-radiatively when they touch a quenching site during their lifetime. The inputs of the simulation are the sample morphology, the measured PL decay time of the pristine polymer film, the measured PL decay time of the specific polymer–PCBM blend, and the PCBM volume fraction in that sample. The only fitting parameter is the exciton diffusion coefficient. As output we get a PL decay, that is, the number of radiatively decayed excitons *versus* time. The simulation is repeated with the adjusted fitting parameter until the modeled and experimental PL decays converge, resulting in the value of exciton diffusion length.

A cubic simulation box with the edge length of 50 nm and periodic boundary conditions is considered to be a continuous medium of polymer phase, in which PCBM quenchers are placed. PCBM molecules are approximated as balls of 1 nm in diameter. Two types of morphologies have been considered, intimate mixture and phase separated PCBM clusters of a certain size. The intimate mixture is modeled by randomly placing PCBM

molecules into the simulation box. A cluster of N molecules is modeled by a center molecule with $N − 1$ nearest neighbors in the triclinic crystal structure of PCBM.[49] The overlapping configurations are not accepted when randomly placing a new quencher or cluster into the box. A Boolean 3D grid of 0.05 nm pitch size is superimposed with the simulation box. Each 3D cell of the grid is given the value *true* or *false* if it overlaps or not with a PCBM molecule. Excitons are described as balls of 1 nm diameter in our Monte Carlo simulation. Since they interact only with quenchers, we can simplify the exciton representation to point particles by increasing the quencher size by the exciton radius. The spatial coordinates of the excitons are not restricted to the Boolean grid nodes.

The use of such a simple[50–52] simulation to model exciton diffusion is justified at room temperature, when exciton hopping in conjugated polymers can be described by normal diffusion:[19,53,54]

$$\frac{\partial n}{\partial t} = D\nabla^2 n - \frac{n}{t}, \qquad (1)$$

where n is the exciton density, D is the diffusion coefficient, and τ is the PL decay time in a pristine polymer film. According to the Einstein's theory of random walks normal diffusion can be modeled as a random walk with constant step size.[29,55–58] For each time iteration δt every exciton is moved in a random 3D direction for a fixed distance δs, which is bound to the diffusion coefficient D by a relationship:

$$D = \frac{\delta s^2}{6\delta t} \qquad (2)$$

The time interval δt is chosen such that δs is several times smaller than the typical quencher size. The exciton diffusion length L_D is then given by the following expression:

$$L_D = \sqrt{aD\tau} \qquad (3)$$

where a depends on the dimensionality of the diffusion process. In the literature about exciton diffusion length measurements the value of a is often considered to be 3 for 3D diffusion. To have our values directly comparable to the previously reported exciton diffusion lengths we set here $a = 3$. However, it is important to note that the value of a of 6 corresponds to the true root mean square displacement in 3D.[59] The exciton is considered to be quenched if its new position overlaps with a grid cell that values *true*. Radiative recombination is assumed if an exciton i has not been quenched after time t_i, which had been fixed at the beginning of the simulation by:

$$t_i = -\tau\ln(w_i), \qquad (4)$$

where w_i is a random number between 0 and 1.

Fig. 3 illustrates the measured PL decays (dotted lines) of polymer:PCBM blends with a PCBM volume fraction of 0.05% for P3HT, C–PCPDTBT and Si–PCPDTBT. The PL decays, which were modeled with the Monte Carlo simulation, are depicted as solid lines. Our model fits the experimental data remarkably well and results in the values of the exciton diffusion coefficient of 2.2×10^{-4}, 27×10^{-4} and 9×10^{-4} cm^2 s^{-1} that correspond to the diffusion length of 5.5, 10.8 and 9.8 nm in P3HT, C–PCPDTBT and Si–PCPDTBT, respectively. An
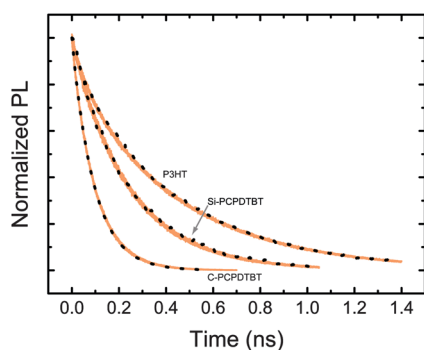
Fig. 3 Fitting of experimentally measured PL decays (dotted lines) of polymer–PCBM blends with Monte Carlo simulation (solid lines). The volume fraction of PCBM was 0.05% in all three blends. Data were normalized to their maximum value at time zero.

"intimate mixture" blend morphology was assumed when modeling these PL decays; we will verify this assumption below. PL decays of blends with other volume fractions were also modeled resulting in *average values* of exciton diffusion coefficients and lengths of $(2.2 \pm 0.3) \times 10^{-4}$ cm^2 s^{-1} and 5.4 ± 0.7 nm in P3HT; $(26 \pm 3) \times 10^{-4}$ cm^2 s^{-1} and 10.6 ± 0.6 nm in C–PCPDTBT; and $(11 \pm 2) \times 10^{-4}$ cm^2 s^{-1} and 10.5 ± 1 nm in Si–PCPDTBT, respectively. The error is the standard deviation in the mean value. The exciton diffusion length in P3HT has been previously reported in the range of 3 and 8.5 nm.[4,12,13,32] Our measurements result in 5.4 nm, which is in agreement with the literature and confirms the validity of our method.

PL decay times of samples of various PCBM fractions can be compared using the relative quenching efficiency Q that is defined as:

$$Q = 1 - \frac{\int \mathrm{PL_{blend}} dt}{\int \mathrm{PL_{pristine}} dt}, \qquad (5)$$

where $\mathrm{PL_{blend}}$ and $\mathrm{PL_{pristine}}$ are normalized to the value at time zero PL decays of a polymer–PCBM blend and pristine polymer, respectively. Nearly zero values of Q indicate that the exciton quenching is insignificant, which is typical for low concentrations of quenching molecules. At high PCBM concentrations most of the excitons are quenched, resulting in a short PL decay time and a close to unity values of Q.

Fig. 4 shows the measured relative quenching efficiency *versus* PCBM volume fraction in polymer–PCBM blends (circles). The solid lines were modeled using the Monte Carlo simulation by setting previously extracted exciton diffusion length for each material and assuming the blend morphology of intimate mixture. The measured data of C–PCPDTBT (Fig. 4a) are excellently described by the simulated curve in all the studied range of PCBM volume fractions. The dotted lines were modeled by setting the exciton diffusion length two nanometres above and below 10.6 nm to demonstrate high sensitivity of the relative quenching efficiency to the exciton diffusion length. Fig. 4b and c show that in the case of Si–PCPDTBT and P3HT the solid line follows the experimental data points only up to a PCBM volume fraction of 0.3% and 0.8%, respectively. Deviation from the measured values is observed for samples of higher PCBM
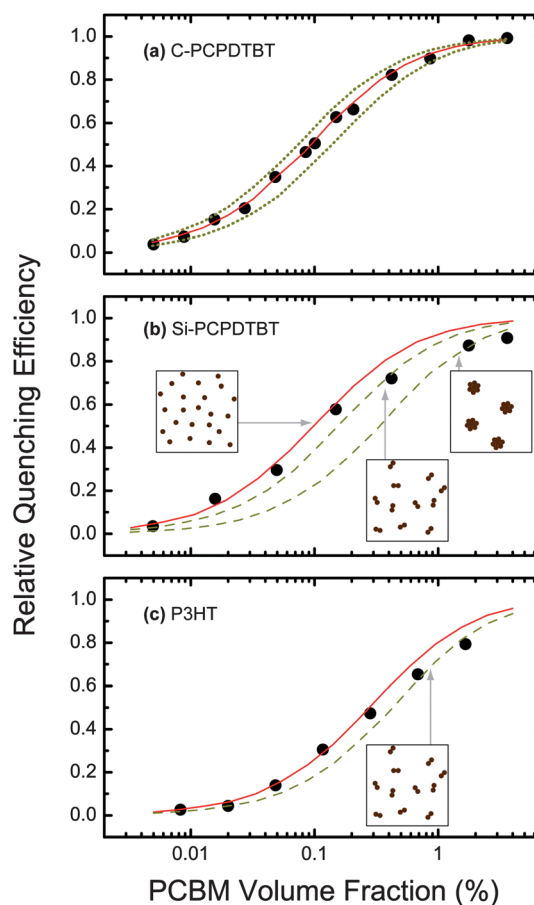

Fig. 4 Measured (circles) and modeled (lines) dependencies of relative quenching efficiency *versus* volume fraction of polymer–PCBM blends. Solid lines represent the fitting of the experimental data with Monte Carlo simulation by setting the blend morphology of intimate mixture. (a) C–PCPDTBT. The fitting yields $L_D = 10.6$ nm (solid line). The dotted lines were modeled assuming the same blend morphology, but with exciton diffusion lengths of two nanometres above and below 10.6 nm. (b) Si–PCPDTBT and (c) P3HT. The fitting results in exciton diffusion lengths of 10.5 and 5.4 nm, respectively (solid lines). The dashed lines were modeled assuming the phase separated morphology of two or seven PCBM molecules per cluster. The insets schematically show these morphologies. The total number of PCBM molecules (black dots) is the same in each inset.

content. The dashed lines are modeled assuming blend morphologies, in which PCBM molecules form clusters of two and seven molecules per cluster.

The deviation between modeled curve (solid lines) and experimental data points (circles) in Fig. 4b and c can be explained by the cluster formation in the polymer–PCBM blends. It is reasonable to assume that the formation of clusters during the solvent evaporation is more likely in blends of higher PCBM fractions. An increase of the cluster size results in the reduction of the interfacial area between polymer and PCBM. Consequently the relative quenching efficiency is smaller in the phase separated sample as compared to the intimately mixed blends of the same PCBM fraction. Indeed, the experimental data at higher volume fractions are much better described by the simulation, in which PCBM molecules are set to form clusters (dashed lines in Fig. 4b and c). Small clusters of two PCBM molecules are formed

in P3HT at PCBM volume fractions in the range of 0.8–1.1%. In the case of Si–PCPDTBT the cluster size gradually increases from two to seven molecules per cluster upon increasing PCBM volume fraction from 0.3% to 3%.

Contrarily, the MC simulation accurately describes the experimentally acquired data in C–PCPDTBT:PCBM blends assuming the formation of the intimate mixture (Fig. 4a). Therefore we conclude that PCBM molecules do not form clusters in C–PCPDTBT in the studied concentration range. Formation of clusters would be indicated by the deviation between the modeled and experimental dependencies at higher PCBM concentrations. One can imagine that fullerene molecules could form clusters of fixed size in the whole concentration range. For instance, if PCBM molecules in blends with C–PCPDTBT would form dimers, then the obtained value for the exciton diffusion length of 10.6 nm would be underestimated. The modeling of the experimental data (Fig. 4a) assuming the dimer morphology results in 13.6 nm (not shown in Fig. 4a), which is roughly $\sqrt[3]{2}$ times the above obtained value of the exciton diffusion length. It is important to note, however, that cluster formation of constant size at each PCBM concentration within the range of three orders of magnitude is highly improbable.

Both, regio-regular P3HT and Si–PCPDTBT are known to form polycrystalline domains,[40,60] while thin films of C–PCPDTBT are amorphous if processed without additives.[40,61–64] Naturally, PCBM molecules are excluded from the polycrystalline domains of P3HT and Si–PCPDTBT leading to phase separation, which we observe as formation of PCBM clusters. We did not detect phase separation in C–PCPDTBT:PCBM blends that is consistent with the amorphous character of this polymer.

Remarkably, the modeled curves in Fig. 4 do not cross in the intermediate concentration range, but rather replicate each other by a translation along the horizontal axis. Therefore we can summarize our methodology as follows: if the experimental data can be described by one of the curves then the quencher molecules form either an intimate mixture with the polymer or clusters of fixed size in the whole concentration range. The latter option is unlikely because the cluster formation probability is increasing with the concentration of quenchers. If the measured relative quenching efficiency grows with the PCBM volume fraction more slowly than a typical modeled curve, then quenchers form larger phase separated domains in that concentration range.

The developed methodology of exciton diffusion measurement has numerous advantages as compared to other techniques. The only fitting parameter is the exciton diffusion length; the model does not require assumptions, for instance, about the exciton–exciton annihilation cross-section.[11,13,30] The measured exciton diffusion length corresponds to the diffusion in three dimensions, which is the case in the bulk heterojunction solar cells. The effects at interfaces of thin films can be safely neglected because the samples are much thicker than the exciton diffusion length. The exciton density variations due to optical interference and light absorption do not influence the PL decay in the blends because samples are isotropic and low exciton densities have been induced—well below 10^{15} cm^{-3}—which are insufficient for the considerable exciton–exciton annihilation. The simplicity of sample preparation and experimental methods makes it practical to systematically measure and compare exciton diffusion length

in a large number of materials. Finally, we can access the polymer-quencher morphology of low quencher concentrations using the MC simulation. To the best of our knowledge, this question has not been addressed before in the PCBM concentration range of 0.01–5 wt%.

Interestingly, the silicon bridged PCPDTBT shows the same exciton diffusion length as the carbon bridged material, while the exciton diffusion coefficient is about two times smaller in Si–PCPDTBT. Mathematically such a contrast is possible due to the fact that PL decay time of the silicon-bridged polymer in pristine film is about two times longer than PL decay time of the carbon bridged one (see eqn (3)). A similar result has been shown by Markov et al. in a family of poly(p-phenylene vinylene) derivatives, in which increase of the exciton diffusion coefficient was compensated by the decrease of the PL decay time leading to the same values of the exciton diffusion length.[28] Although Si–PCPDTBT and C–PCPDTBT have the same exciton diffusion length, the performance of the former material in bulk heterojunction solar cells is higher.[40] Thus other factors such as blend morphology, charge carrier mobility and different loss mechanisms[40,63,65,66] are responsible for higher efficiency of solar cells in the case of these two specific polymers.

4. Conclusions

Using a newly developed method we found that PCBM molecules form intimate mixtures with C–PCPDTBT in blends with fullerene concentration ranging from 0.01 to 5 wt%. Phase separated domains have been detected in Si–PCPDTBT and P3HT at concentrations above 0.9 wt% and 1.8 wt%, respectively. The knowledge about the blend morphology allows us to model 3D diffusion and accurately determine the exciton diffusion coefficients and diffusion lengths of $(26 \pm 3) \times 10^{-4}$ cm^2 s^{-1} and 10.6 ± 0.6 nm in C–PCPDTBT; $(11 \pm 2) \times 10^{-4}$ cm^2 s^{-1} and 10.5 ± 1 nm in Si–PCPDTBT; and $(2.2 \pm 0.5) \times 10^{-4}$ cm^2 s^{-1} and 5.4 ± 0.7 nm in P3HT. Since the exciton diffusion length is the same in both narrow band gap polymers, the higher performances of Si–PCPDTBT are not correlated to the process of exciton diffusion. Compared to other techniques, the proposed method for exciton diffusion measurement has numerous advantages and is suitable for systematic studies in a large number of materials.

References

1 M. Campoy-Quiles, T. Ferenczi, T. Agostinelli, P. G. Etchegoin, Y. Kim, T. D. Anthopoulos, P. N. Stavrinou, D. D. C. Bradley and J. Nelson, Nat. Mater., 2008, 7, 158–164.
2 M. A. Green, K. Emery, Y. Hishikawa and W. Warta, Prog. Photovoltaics, 2011, 19, 84–92.
3 P. Peumans, A. Yakimov and S. R. Forrest, J. Appl. Phys., 2003, 93, 3693–3723.
4 C. Goh, S. R. Scully and M. D. McGehee, J. Appl. Phys., 2007, 101, 114503.

5 S.-B. Rim, R. F. Fink, J. C. Schöneboom, P. Erk and P. Peumans, *Appl. Phys. Lett.*, 2007, **91**, 173504.
6 L. D. A. Siebbeles, A. Huijser and T. J. Savenije, *J. Mater. Chem.*, 2009, **19**, 6067.
7 Y. Terao, H. Sasabe and C. Adachi, *Appl. Phys. Lett.*, 2007, **90**, 103515.
8 V. Bulovic and S. R. Forrest, *Chem. Phys. Lett.*, 1995, **238**, 88–92.
9 W. A. Luhman and R. J. Holmes, *Adv. Funct. Mater.*, 2011, **21**, 764–771.
10 H. Wang, H.-Y. Wang, B.-R. Gao, L. Wang, Z.-Y. Yang, X.-B. Du, Q.-D. Chen, J.-F. Song and H.-B. Sun, *Nanoscale*, 2011, **3**, 2280.
11 S. Cook, H. Liyuan, A. Furube and R. Katoh, *J. Phys. Chem. C*, 2010, **114**, 10962–10968.
12 L. Lüer, H.-J. Egelhaaf, D. Oelkrug, G. Cerullo, G. Lanzani, B.-H. Huisman and D. de Leeuw, *Org. Electron.*, 2004, **5**, 83–89.
13 P. E. Shaw, A. Ruseckas and I. D. W. Samuel, *Adv. Mater.*, 2008, **20**, 3516–3520.
14 K. Masuda, Y. Ikeda, M. Ogawa, H. Benten, H. Ohkita and S. Ito, *ACS Appl. Mater. Interfaces*, 2010, **2**, 236–245.
15 S. Cook, A. Furube, R. Katoh and L. Han, *Chem. Phys. Lett.*, 2009, **478**, 33–36.
16 H. Najafov, B. Lee, Q. Zhou, L. C. Feldman and V. Podzorov, *Nat. Mater.*, 2010, **9**, 938–943.
17 R. R. Lunt, J. B. Benziger and S. R. Forrest, *Adv. Mater.*, 2010, **22**, 1233–1236.
18 R. R. Lunt, N. C. Giebink, A. A. Belak, J. B. Benziger and S. R. Forrest, *J. Appl. Phys.*, 2009, **105**, 053711.
19 O. V. Mikhnenko, F. Cordella, A. B. Sieval, J. C. Hummelen, P. W. M. Blom and M. A. Loi, *J. Phys. Chem. B*, 2008, **112**, 11601–11604.
20 C. L. Yang, Z. K. Tang, W. K. Ge, J. N. Wang, Z. L. Zhang and X. Y. Jian, *Appl. Phys. Lett.*, 2003, **83**, 1737–1739.
21 T. Stubinger and W. Brutting, *J. Appl. Phys.*, 2001, **90**, 3632–3641.
22 J. J. M. Halls, K. Pichler, R. H. Friend, S. C. Moratti and A. B. Holmes, *Appl. Phys. Lett.*, 1996, **68**, 3120–3122.
23 B. A. Gregg, J. Sprague and M. W. Peterson, *J. Phys. Chem. B*, 1997, **101**, 5362–5369.
24 A. Haugeneder, M. Neges, C. Kallinger, W. Spirkl, U. Lemmer, J. Feldmann, U. Scherf, E. Harth, A. Gügel and K. Müllen, *Phys. Rev. B: Condens. Matter*, 1999, **59**, 15346.
25 M. Theander, A. Yartsev, D. Zigmantas, V. Sundström, W. Mammo, M. R. Andersson and O. Inganäs, *Phys. Rev. B: Condens. Matter*, 2000, **61**, 12957.
26 Y. Wu, Y. C. Zhou, H. R. Wu, Y. Q. Zhan, J. Zhou, S. T. Zhang, J. M. Zhao, Z. J. Wang, X. M. Ding and X. Y. Hou, *Appl. Phys. Lett.*, 2005, **87**, 044104.
27 D. E. Markov, E. Amsterdam, P. W. M. Blom, A. B. Sieval and J. C. Hummelen, *J. Phys. Chem. A*, 2005, **109**, 5266–5274.
28 D. E. Markov, C. Tanase, P. W. M. Blom and J. Wildeman, *Phys. Rev. B: Condens. Matter Mater. Phys.*, 2005, **72**, 045217.
29 Y. C. Zhou, Y. Wu, L. L. Ma, J. Zhou, X. M. Ding and X. Y. Hou, *J. Appl. Phys.*, 2006, **100**, 023712.
30 A. J. Lewis, A. Ruseckas, O. P. M. Gaudin, G. R. Webster, P. L. Burn and I. D. W. Samuel, *Org. Electron.*, 2006, **7**, 452–456.
31 S. R. Scully and M. D. McGehee, *J. Appl. Phys.*, 2006, **100**, 034907.
32 J. E. Kroeze, T. J. Savenije, M. J. W. Vermeulen and J. M. Warman, *J. Phys. Chem. B*, 2003, **107**, 7696–7705.
33 C. Breyer, M. Vogel, M. Mohr, B. Johnev and K. Fostiropoulos, *Phys. Status Solidi B*, 2006, **243**, 3176–3180.
34 O. V. Mikhnenko, F. Cordella, A. B. Sieval, J. C. Hummelen, P. W. M. Blom and M. A. Loi, *J. Phys. Chem. B*, 2009, **113**, 9104–9109.
35 D. Qin, P. Gu, R. S. Dhar, S. G. Razavipour and D. Ban, *Phys. Status Solidi A*, 2011, **208**, 1967–1971.
36 D. E. Markov and P. W. M. Blom, *Phys. Rev. B: Condens. Matter Mater. Phys.*, 2006, **74**, 085206.
37 B. Y. Balagurov and V. G. Vaks, *JETP Lett.*, 1973, **65**, 1939–1946.
38 L. J. Rothberg, M. Yan, F. Papadimitrakopoulos, M. E. Galvin, E. W. Kwock and T. M. Miller, *Synth. Met.*, 1996, **80**, 41–58.
39 M. Yan, L. J. Rothberg, F. Papadimitrakopoulos, M. E. Galvin and T. M. Miller, *Phys. Rev. Lett.*, 1994, **73**, 744.
40 M. C. Scharber, M. Koppe, J. Gao, F. Cordella, M. A. Loi, P. Denk, M. Morana, H.-J. Egelhaaf, K. Forberich, G. Dennler, R. Gaudiana, D. Waller, Z. Zhu, X. Shi and C. J. Brabec, *Adv. Mater.*, 2010, **22**, 367–370.
41 M. Matsumoto and T. Nishimura, *ACM Trans. Model. Comput. Simul.*, 1998, **8**, 3–30.
42 "Pseudo random number generators", can be found under http://www.agner.org/random/.
43 Software for Monte Carlo simulation can be downloaded at http://mikhnenko.com/eDiffusion/.
44 T. J. Prosa, M. J. Winokur, J. Moulton, P. Smith and A. J. Heeger, *Macromolecules*, 1992, **25**, 4364–4372.
45 J. Mårdalen, E. J. Samuelsen, O. R. Gautun and P. H. Carlsen, *Solid State Commun.*, 1991, **77**, 337–339.
46 M. M. Erwin, J. McBride, A. V. Kadavanich and S. J. Rosenthal, *Thin Solid Films*, 2002, **409**, 198–205.
47 T. Yamamoto, Q. Fang and T. Morikita, *Macromolecules*, 2003, **36**, 4262–4267.
48 C. W. T. Bulle-Lieuwma, W. J. H. van Gennip, J. K. J. van Duren, P. Jonkheijm, R. A. J. Janssen and J. W. Niemantsverdriet, *Appl. Surf. Sci.*, 2003, **203–204**, 547–550.
49 M. T. Rispens, A. Meetsma, R. Rittberger, C. J. Brabec, N. S. Sariciftci and J. C. Hummelen, *Chem. Commun.*, 2003, 2116.
50 T. A. Papadopoulos, L. Muccioli, S. Athanasopoulos, A. B. Walker, C. Zannoni and D. Beljonne, *Chem. Sci.*, 2011, **2**, 1025–1032.
51 S. Athanasopoulos, E. Hennebicq, D. Beljonne and A. B. Walker, *J. Phys. Chem. C*, 2008, **112**, 11532–11538.
52 A. A. Ovchinnikov and V. V. Atrazhev, *Phys. Lett. A*, 1999, **256**, 217–220.
53 F. B. Dias, K. T. Kamtekar, T. Cazati, G. Williams, M. R. Bryce and A. P. Monkman, *ChemPhysChem*, 2009, **10**, 2096–2104.
54 M. Anni, M. E. Caruso, S. Lattante and R. Cingolani, *J. Chem. Phys.*, 2006, **124**, 134707.
55 S. B. Lee, I. C. Kim, C. A. Miller and S. Torquato, *Phys. Rev. B*, 1989, **39**, 11833.
56 M. R. Riley, F. J. Muzzio, H. M. Buettner and S. C. Reyes, *Phys. Rev. E: Stat. Phys., Plasmas, Fluids, Relat. Interdiscip. Top.*, 1994, **49**, 3500.
57 M. R. Riley, H. M. Buettner, F. J. Muzzio and S. C. Reyes, *Biophys. J.*, 1995, **68**, 1716–1726.
58 J. A. Anta, *Energy Environ. Sci.*, 2009, **2**, 387.
59 M. Pope and C. E. Swenberg, *Electronic Processes in Organic Crystals and Polymers*, Oxford University Press, 2nd edn, 1999.
60 X. Yang, J. Loos, S. C. Veenstra, W. J. H. Verhees, M. M. Wienk, J. M. Kroon, M. A. J. Michels and R. A. J. Janssen, *Nano Lett.*, 2005, **5**, 579–583.
61 J. Peet, J. Y. Kim, N. E. Coates, W. L. Ma, D. Moses, A. J. Heeger and G. C. Bazan, *Nat. Mater.*, 2007, **6**, 497–500.
62 D. Di Nuzzo, A. Aguirre, M. Shahid, V. S. Gevaerts, S. C. J. Meskers and R. A. J. Janssen, *Adv. Mater.*, 2010, **22**, 4321–4324.
63 M. Morana, H. Azimi, G. Dennler, H.-J. Egelhaaf, M. Scharber, K. Forberich, J. Hauch, R. Gaudiana, D. Waller, Z. Zhu, K. Hingerl, S. S. van Bavel, J. Loos and C. J. Brabec, *Adv. Funct. Mater.*, 2010, **20**, 1180–1188.
64 M. Morana, M. Wegscheider, A. Bonanni, N. Kopidakis, S. Shaheen, M. Scharber, Z. Zhu, D. Waller, R. Gaudiana and C. Brabec, *Adv. Funct. Mater.*, 2008, **18**, 1757–1766.
65 D. Jarzab, F. Cordella, J. Gao, M. Scharber, H. Egelhaaf and M. A. Loi, *Adv. Energy Mater.*, 2011, **1**, 604–609.
66 C. V. Hoven, X.-D. Dang, R. C. Coffin, J. Peet, T.-Q. Nguyen and G. C. Bazan, *Adv. Mater.*, 2010, **22**, E63–E66.

This journal is © The Royal Society of Chemistry 2012

Energy Environ. Sci., 2012, **5**, 6960–6965 | 6965